Am J Transl Res 2020;12(8):4290-4301
www.ajtr.org /ISSN:1943-8141/AJTR0108695

Original Article

TMT-based proteomic analysis reveals the effects of chloroquine on human podocytes

Yulin Kang[1], Helen Ka-Wai Law[2], Yanyang Zhang[1], Ying Wu[1], Guang-Hua Zhu[1], Moin Ahson Saleem[3], Wen-Yan Huang[1]

[1]Department of Nephrology and Rheumatology, Shanghai Children's Hospital, Shanghai Jiao Tong University, Shanghai 200062, China; [2]Department of Health Technology and Informatics, Faculty of Health and Social Science, The Hong Kong Polytechnic University, Hunghom, Hong Kong 999077, China; [3]Children's Renal Unit, University of Bristol, Bristol, BS2 8BJ, United Kingdom

Received February 4, 2020; Accepted July 4, 2020; Epub August 15, 2020; Published August 30, 2020

Abstract: Chloroquine (CQ) is an antimalarial drug widely used in rheumatic, immunological and infectious diseases. CQ is also a well-known autophagy inhibitor. It slows the progression of renal injury in patients with rheumatology diseases. Long-term CQ treatment could also damage podocytes which are highly differentiated cells wrapping the glomerular capillary to maintain renal filtration. However, the related underlying mechanism remains unclear. The effects of CQ treatment on podocytes need to be elucidated. Our results showed that CQ diminished cell motility and disrupted actin cytoskeleton in human podocytes in vitro. Totally 210 up-regulated and 67 down-regulated differentially expressed proteins (DEPs) were identified after CQ treatment in podocytes by using tandem mass tag (TMT)-labeled quantitative proteomics analysis. Gene Ontology (GO) analysis revealed that proteins mainly functioned in cell motility, cell adhesion, localization of cells and response to external stimulus. Kyoto Encyclopedia of Genes and Genomes (KEGG) enrichment showed that DEPs were predominantly associated with lysosome, cell adhesion molecules (CAMs) and cytokine-cytokine receptor interaction. Protein-protein interaction (PPI) analysis revealed that syndecan-4 was the core protein in regulating podocyte adhesion among differentially expressed CAMs. Moreover, activated RhoA, Cdc42 and Rac1 decreased after CQ treatment. Taken together, our findings suggested that CQ could alter the stability of podocyte cytoskeleton. Proteomic analysis revealed important molecules for understanding the effects of CQ on human podocytes.

Keywords: Podocyte, chloroquine, autophagy, actin cytoskeleton

Introduction

Podocytes are highly differentiated mesenchymal-like cells which have three different morphological and functional parts: cell body, major process and foot process. Foot processes of adjacent podocytes interdigitate and form the outside layer of renal filtration barrier [1]. The cell body and major process of podocyte rely on microtubules and intermediate filaments for keeping normal morphology, while foot process is supported by the actin cytoskeleton [2]. Foot process contains highly ordered parallel and contractile filamentous actin network. This actin cytoskeleton is cross-linked and bundled by several proteins such as alpha-actinin-4 and synaptopodin [3, 4]. The normal morphology and function of foot process bases on intact actin cytoskeleton. Instability of actin cytoskeleton contributes to proteinuria.

Proteinuria is the most common symptom if podocytes undergo detachment or foot processes effacement which is marked with depolymerized actin cytoskeleton [2, 5]. For instance, minimal change nephrotic syndrome is featured by heavy proteinuria due to foot process effacement [6]. To emphasize the importance of podocyte in glomerular diseases, the term of podocytopathy has been created for describing the podocyte-injury related diseases [7]. Podocytopathy could result from medication, gene mutation and immunological disorders [8-10].

CQ is an anti-malarial drug that has multiple properties, such as anti-inflammation, anti-

thrombus and anti-infection. Hence, it is widely used in rheumatic, immunological and infectious diseases [11]. CQ and its analogues show beneficial effects in patients with lupus nephritis as they slow the progression of renal injury and decrease the complications of infection, hypertension and thrombotic events [12]. Good safety profile was noted as only a small portion of patients receiving long-term CQ treatment has mild or moderate side effects including ocular toxicity and gastrointestinal manifestations [13]. Toll-like receptor 3 (TLR3)/IFN-β signaling could be attenuated by CQ in human mesangial cells [14]. It may partially explain the efficacy of CQ in lupus nephritis. However, little is known about the effects of CQ treatment on human podocytes. To date, only one case report showed that CQ treatment induces phospholipidosis in podocytes mimicking Fabry disease as plenty of zebra bodies could be visualized [15]. In addition, CQ is a well-known autophagy inhibitor. It has been reported that autophagic gene deficient cell presents with depolymerization of actin cytoskeleton [16]. It remains unclear whether CQ disrupts the stability of podocyte cytoskeleton.

In this study, our data showed that CQ could diminish cell motility and disrupt actin cytoskeleton of human podocytes. We performed TMT-based quantitative proteomic analysis to identify differentially expressed proteins (DEPs) in CQ-treated human podocytes. This study firstly revealed the impact of CQ treatment on the stability of podocyte cytoskeleton. It not only helps to elucidate the pathogenesis of podocytopathy, but may also explain the efficacy and side effects of CQ in treating rheumatic and immunological diseases.

Materials and methods

Cell culture

Conditionally immortalized human podocytes AB8/13 were cultured in RPMI 1640+10% fetal bovine serum (Thermo Fisher Scientific) as described previously [17]. Cells proliferated at non-permissive temperature (33°C) with the addition of Insulin-Transferrin-Selenium (Thermo Fisher Scientific) and differentiated in permissive temperature (37°C) for 12 days. Fully differentiated human podocytes were treated with Chloroquine (CQ, 25 μM) (Sigma-Aldrich). The optimum concentration of CQ has been titrated in our previous studies [18, 19].

Immunofluorescence analysis

Fully differentiated podocytes with 80% confluency in 24-well plates were treated with CQ (25 μM) for 24 h and 48 h. 4% paraformaldehyde was used for fixing podocytes. After blocking with PBS +2% BSA, F-actin and nucleus were stained with Alexa Fluor 594 Phalloidin (Thermofisher Scientific) and ProLong Gold Antifade Reagent with DAPI (Cell signaling Technology) respectively. Podocytes were visualized under confocal microscopy (EZ-C1, Nikon Instrument, Japan). The percentage of podocytes with disrupted cytoskeleton was quantified as the previous study described [18]. At least 100 cells were scored in each of six independent experiments.

Migration assay

Fully differentiated podocytes in 6-well plates were scratched by two strokes with a sterile 0.4 mm 200 μl Gilson style extension length tip. Then, cells were treated with CQ (25 μM) for 8 h. Two researchers counted the number of podocytes migrating into the gap independently as described before [19].

TMT-based quantitative proteomic analysis

Fully differentiated podocytes with 80% confluency were treated with CQ (25 μM) for 24 h. Podocytes were lysed in SDT buffer (4% SDS, 100 mM DTT and 150 mM Tris-HCl pH 8.0). The concentration of supernatant was measured with BCA Protein Assay Kit (Bio-Rad, USA) after centrifuging at 14000 g for 40 minutes. Proteins were purified after repeated ultrafiltration (Microcon units, 10 kD) with UA buffer (8M Urea, 150 mM Tris-HCl pH 8.0). 100 ul iodoacetamide was used to block reduced cysteine residues. Then, samples were put in darkness for 30 min incubation. The filters were washed with UA buffer three times and TEAB buffer (100 mM) twice. Eventually, protein suspensions were digested overnight at 37°C by using 4 μg trypsin (Promega) in 40 μl TEAB buffer. Peptides were collected by filtration. Peptide content was estimated by UV light spectral density at 280 nm. Peptide mixture of each sample (100 μg) was labeled with TMT reagent according to the manufacturer's instructions (Thermo Fisher Scientific). TMT-labeled digest samples were fractionated by Pierce high pH reversed-phase fractionation kit (Thermo scientific) based on an increasing acetonitrile step-gradi-

Table 1. The real-time PCR primers of 6 key cell adhesion molecules (CAMs)

Gene name	Protein IDs	Protein name	Sequence	Size (bp)
ITGB8	P26012	Integrin beta-8	Forward: 5' CCAGGAGCCGAAGCTAATT 3' Reverse: 5' CGTATGAGCCAAATCCAAGAC 3'	190
CLDN1	O95832	Claudin-1	Forward: 5' GAGGATGGCTGTCATTGGG 3' Reverse: 5' GGTGTTGGGTAAGAGGTTGTTT 3'	240
SDC4	P31431	Syndecan-4	Forward: 5' AGCCAAGTCCCCACCGA 3' Reverse: 5' CAAAGAGGATGCCCACGAT 3'	193
CLDN4	O14493	Claudin-4	Forward: 5' CCTCGTCATCATCAGCATCA 3' Reverse: 5' GACACCGGCACTATCACCAT 3'	165
VCAM1	P19320	Vascular cell adhesion protein 1	Forward: 5' TACAACCGTCTTGGTCAGCC 3' Reverse: 5' TTCCTTCACATAAATAAACCCCA 3'	206
L1CAM	P32004	Neural cell adhesion molecule L1	Forward: 5' TGCGGACAATCAGACGTACA 3' Reverse: 5' TTGGCATAGGGGAAGAAGC 3'	147
GAPDH	P04406	GAPDH	Forward: 5' TGGGTGTGAACCATGAGAAGT 3' Reverse: 5' TGAGTCCTTCCACGATACCAA 3'	126

ent elution as described before. Peptide mixture was added to a reverse phase trap column (Thermo Scientific Acclaim PepMap100, 100 μm*2 cm, nanoViper C18) connected to the C18-reversed phase analytical column (Thermo Scientific Easy Column, 10 cm long, 75 μm inner diameter, 3 μm resin) in buffer A (0.1% Formic acid). It was separated with a 60 min gradient of 0-50% buffer B (50 min), 50-100% buffer B (5 min), 100% buffer B (5 min) at a flow rate of 300 nl/min which was controlled by IntelliFlow technology. LC-MS/MS analysis was carried out on a Q Exactive mass spectrometer (Thermo Scientific) that was linked to Easy nLC (Proxeon Biosystems, now Thermo Fisher Scientific). TMT-based quantitative proteomic analysis was performed in Shanghai Applied Protein Technology Company (Shanghai, China).

Quantitative real-time PCR

Podocytes were treated with CQ (25 μM) for 12 hours. Total RNA was extracted from podocytes by using Trizol reagent (Invitrogen, Carlsbad, CA) and reversely transcribed to single-stranded cDNA with PrimeScript RT Reagent Kit (Takara Bio, Kyoto, Japan) according to manufacture's instruction. Quantitative real-time PCR was performed in Step One Plus real-time PCR system (ABI, Foster, CA, USA) with 2X SG Fast qPCR Master Mix (High Rox, B639273, BBI). Detection was done in triplicate. Reaction was performed at 95°C for 3 min followed by 45 cycles of denaturation at 95°C for 5 s, annealing at 60°C for 30 s, and extension at 72°C for 30 s. Glyceraldehyde-3-phosphate dehydrogenase (GAPDH) was set as an internal reference. The real-time PCR primers are shown in **Table 1**. Relative mRNA expression was calculated by using the $2^{-\Delta\Delta ct}$ method.

RhoA, Cdc42 and Rac1 G-LISA assay

G-LISA assay kit (Cytoskeleton) was used for measuring GTP bound (activated) RhoA, Cdc42 and Rac1 in human podocytes following the manufacture's protocols. Fully differentiated podocytes with 80% confluency were treated with CQ (25 μM) for 24 h. Cells were harvested using the lysis buffer containing protein inhibitors and the final protein concentration was adjusted to 0.8 mg/L. OD values were measured with the absorbance of 595 nm and represented the expression of activated RhoA, Rac1 and Cdc42.

Statistical analysis and bioinformatics

Data were expressed as mean ± SEM. Non parametric T-test was used for two group's comparison and using the Prism 5.0 Software (GraphPad, San Diego, CA, USA). A p value <0.05 was considered to be statistically significant.

As for bioinformatics in proteome, differential expressed proteins were defined as the ones with 1.2 folds up-regulation or 0.83 folds down-regulation changes (P value <0.05). The protein sequences were aligned to Gene Ontology (GO) Consortium database for GO assignment. The FASTA protein sequences were blasted against the online Kyoto Encyclopedia of Genes and

Genomes (KEGG) database (http://geneontology.org/) and subsequently mapped to KEGG pathways. Protein-protein interaction (PPI) was retrieved from STRING database (http://string-db.org/). The results were visualized and analyzed by using Cytoscape software (http://www.cytoscape.org/, version 3.2.1). Bioinformatics was performed by Shanghai Applied Protein Technology Company (Shanghai, China).

Results

CQ decreased cell motility and disrupted actin cytoskeleton of human podocytes

In glomerulus, podocyte motility is kept at a considerable level [20]. It is an essential process for cleaning proteins deposit in subpodocyte space which covers around 60% of GBM [21, 22]. Thus, podocyte motility serves as a self-cleaning mechanism to ensure the normal filtration. To test whether CQ affects podocyte motility, migration assay was performed in the present study. As shown in **Figure 1A-D**, the number of podocytes migrating into the gap after 8 h CQ treatment decreased significantly.

In our previous study, we found that depolymerization of podocyte actin cytoskeleton caused by puromycin aminonucleoside was deteriorated after autophagy inhibition by CQ at 24 h [18]. For verifying the impact of CQ uniquely on actin cytoskeleton, we treated podocytes with CQ for 24 h and 48 h. As shown in **Figure 1E-H**, the cortical cytoskeleton was formed in podocytes at 24 h and orderly actin-stress fiber organization was lost at 48 h. The percentage of podocytes with disrupted actin cytoskeleton increased significantly after 24 h CQ treatment.

Proteomic analysis identified DEPs in human podocytes after CQ treatment

Totally 5247 proteins were identified based on 34969 unique peptides by TMT-based proteomic analysis. There were 277 DEPs (210 up-regulated and 67 down-regulated) after CQ treatment in podocytes (Supplementary Material-1). DEPs were categorized into biological process, molecular function and cellular component according to GO annotation. As showed in **Figure 2**, response to external stimulus, cell motility, localization of cells, biological adhesion and cell migration were the top 5 biological processes. In the aspect of molecular function, most of DEPs were involving in signaling receptor binding. Additionally, majority of proteins were distributed in cell membrane parts.

To identify the involved signalling pathways, the DEPs were mapped to KEGG pathways. As showed in **Figure 3** and **Table 2**, the top 20 enriched KEGG pathways were listed. The top 5 KEGG pathways basing on the number of involved DEPs were lysosome, proteoglycans in cancer, cytokine-cytokine receptor interaction, cell adhesion molecules (CAMs), complement and coagulation cascades. Since podocyte detachment plays a crucial role in proteinuria diseases, studying the differentially expressed CAMs helps to understand the efficacy and side effects of CQ in renal diseases. Twelve CAMs after CQ treatment are identified as follows: Integrin beta-8 (1.61 folds), Claudin-1 (1.46 folds), Myelin protein zero-like protein 1 (1.42 folds), Receptor-type tyrosine-protein phosphatase F (1.37 folds), Syndecan-4 (1.34 folds), Claudin-4 (1.28 folds), Intercellular adhesion molecule 1 (1.25 folds), Receptor-type tyrosine-protein phosphatase mu (1.24 folds), Vascular cell adhesion protein 1 (1.23 folds), Tumor necrosis factor receptor superfamily member 5 (1.21 folds), Neural cell adhesion molecule L1 (1.2 folds) and CD99 antigen (0.79 folds).

To explore the relationship of DEPs in CQ-treated human podocytes, proteins interaction was constructed by PPI analysis. There were totally 155 nodes and 862 edges in PPI network. Totally 6 CAMs were founded in PPI network: Syndecan-4, Integrin beta-8, Vascular cell adhesion protein 1, Neural cell adhesion molecule L1, Claudin-1 and Claudin-4. Among these CAMs, Syndecan-4 was the core protein in regulating podocyte adhesion (**Figure 4**).

The expression of 6 key CAMs was verified by qPCR

For verifying the expression of 6 CAMs (Syndecan-4, Integrin beta-8, Vascular cell adhesion protein 1, Neural cell adhesion molecule L1, Claudin-1 and Claudin-4) which were illustrated in PPI, their mRNA expression level was measured by qPCR. The data were consistent with that from TMT assay as all of them increased (**Figure 5**).

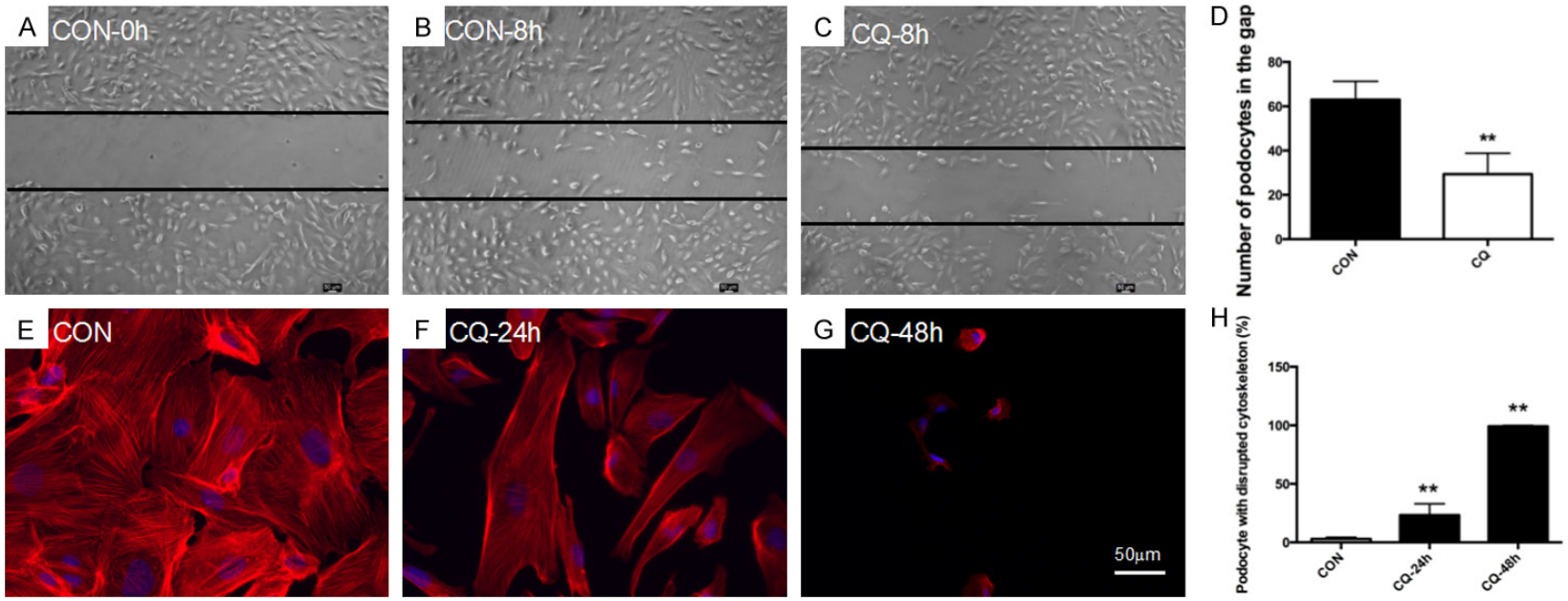

Figure 1. CQ decreased cell motility and disrupted actin cytoskeleton of human podocyte. (A-D) The number of podocytes migrating into the gap was calculated for evaluating podocyte mobility. Podocytes were treated with CQ (25 μM) for 8 hours. The representative images were taken under inverted microscope (50×). It showed that podocyte mobility decreased significantly after CQ treatment. $^{**}P<0.01$ versus CON, n=6. (E-H) CQ disrupted actin cytoskeleton of podocytes. The cortical cytoskeleton was observed in podocytes after treating with CQ (25 μM) for 24 h and orderly arranged actin-stress fiber disappeared at 48 h. Data of statistical analysis showed that the percentage of podocytes with disrupted actin cytoskeleton increased significantly. $^{**}P<0.01$ versus CON, n=6.

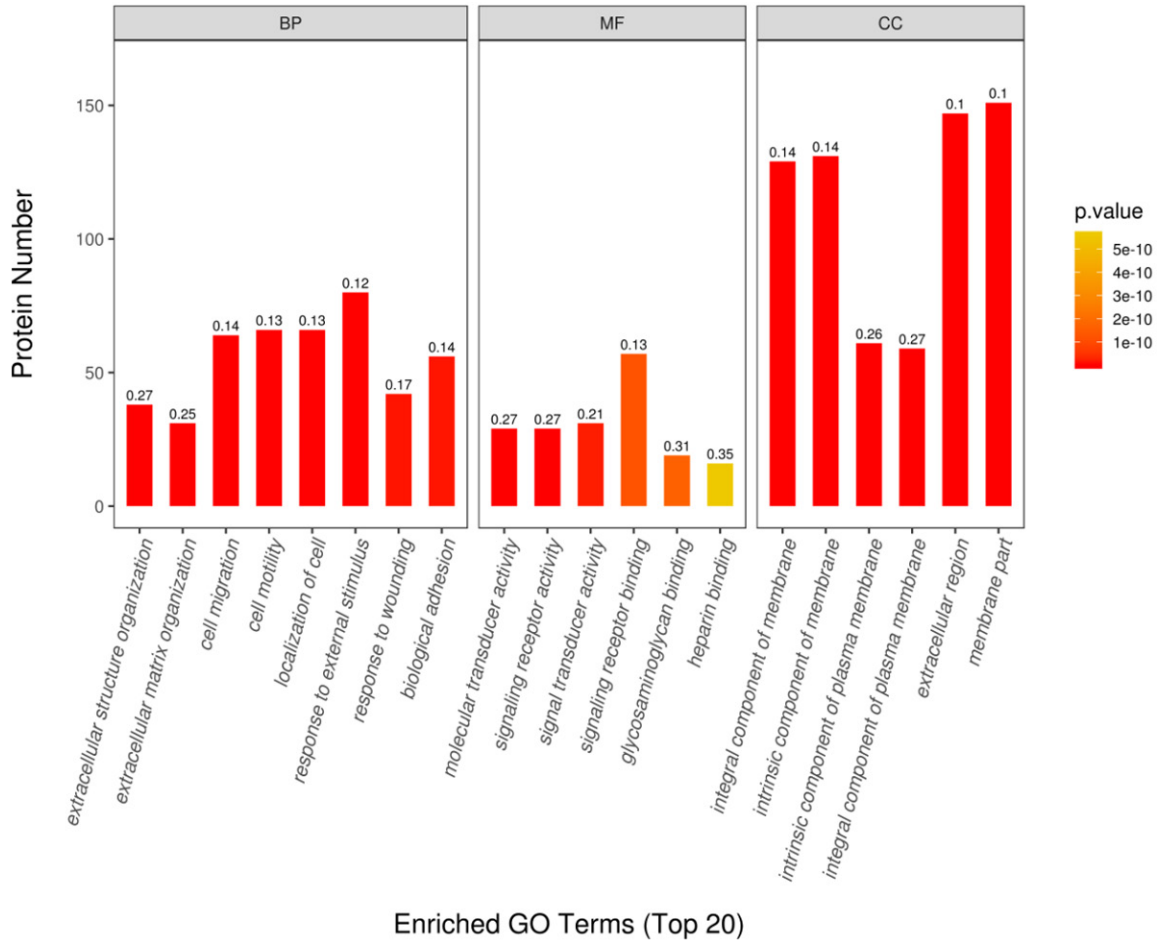

Figure 2. GO annotation of differentially expressed proteins (DEPs) in CQ-treated podocytes. Totally 277 DEPs were identified after CQ treatment in podocytes. They were categorized into biological process (BP), molecular function (MF) and cellular component (*CC*) according to GO annotation. The magnitude of *P* value was indicated by color gradient. The number on the top of column was the rich factor (rich factor ≤1). Top 5 biological processes are response to external stimulus, cell motility, localization of cells, biological adhesion and cell migration. In the aspect of molecular function, most of DEPs were involving in signaling receptor binding. As for cellular component, majority of proteins were distributed in cell membrane parts.

Representative active small GTPases decreased in CQ-treated human podocytes

The RhoA family of small GTPases regulates many cellular processes. RhoA, Rac1 and CDC42 are the representative ones and responsible for maintaining the stability of actin cytoskeleton. It has been known that RhoA participates in the formation of actin stress fibers [23]. Rac1 and Cdc42 are responsible for the formation of lamellipodia and filopodia respectively [24]. To verify whether the actin cytoskeleton disassembly is subject to the changes of these small Rho-GTPases, the active form of RhoA, Rac1 and CDC42 were measured after CQ treatment. As shown in **Figure 6**, active RhoA, Rac1 and CDC42 decreased significantly in podocytes.

Discussion

Podocytes form the outside layer of renal filtration barrier. The stability of actin cytoskeleton architecture in podocyte was crucial for maintaining normal renal filtration. Proteinuria will occur if podocytes detach or actin cytoskeleton undergoes depolymerization. Here we showed the effects of CQ on human podocytes *in vitro*. In addition, TMT-labeled quantitative proteomics approach was used to explore the underlying mechanisms.

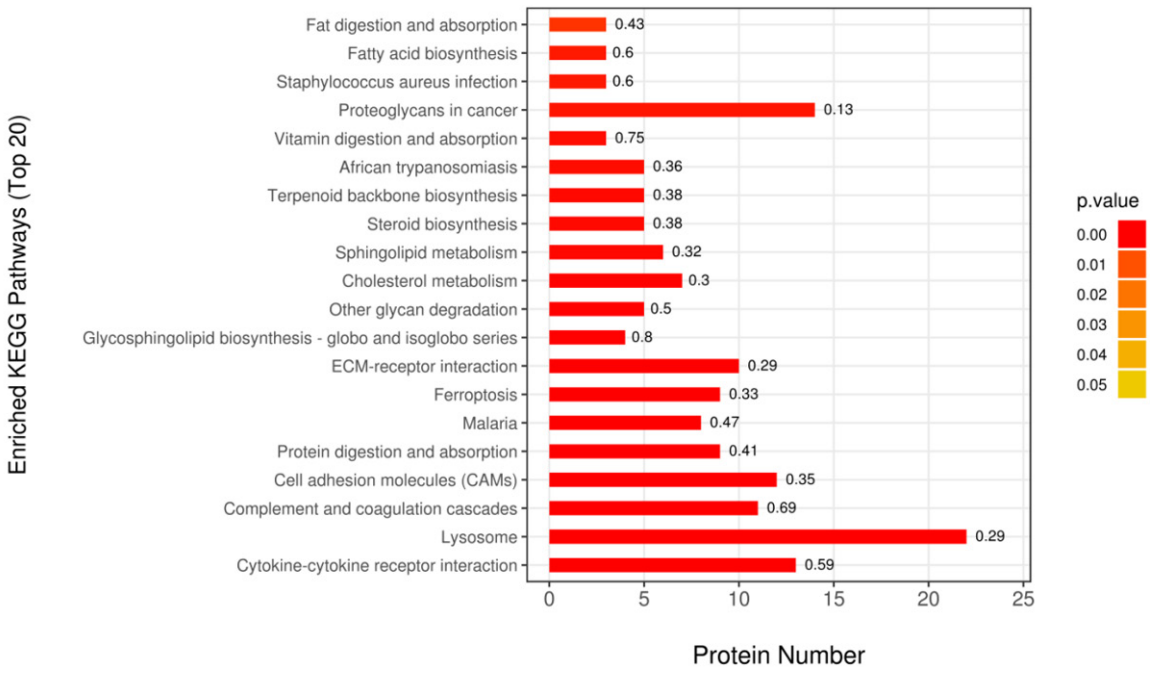

Figure 3. Functional enrichment analysis of DEPs. Top 20 enriched KEGG pathways were identified based on the DEPs in CQ-treated podocytes. The magnitude of *P* value was indicated by color gradient. The number on the top of column was the rich factor (rich factor ≤1).

Our results showed that cell motility decreased in CQ-treated human podocytes. It is well known that increased podocyte motility under harmful stimuli disrupts the normal function of renal filtration barrier [1]. Hence, CQ treatment may alleviate podocyte injury by normalizing cell motility. It may explain why CQ and its analogues show therapeutic effects in lupus nephritis [25]. Moreover, CQ might also strengthen cell adhesion. TMT-labeled quantitative proteomics analysis showed that 12 differentially expressed CAMs were involved in cell adhesion. PPI analysis found that 6 of them had at least one protein-protein interaction. They are Syndecan-4, Integrin beta-8, Vascular cell adhesion protein 1, Neural cell adhesion molecule L1, Claudin-1 and Claudin-4. qPCR data of these 6 proteins were consistent with proteomic results, suggesting that their increased protein expression might be regulated at the transcriptional level. Syndecan-4 is a proteoglycan receptor and plays a key role in regulating podocyte adhesion and motility. Overexpression of Syndecan-4 in podocytes reduces RhoA activity which could decrease the formation of actin stress fibre and podocyte motility [26]. Syndecan-4 increased after CQ treatment, suggesting that it may enhance the adhesion between podocytes and glomerular basement membrane, but diminished podocyte motility. Similarly, the other increased 5 CAMs (Integrin beta-8, Vascular cell adhesion protein 1, Neural cell adhesion molecule L1, Claudin-1 and Claudin-4) could also strengthen cell adhesion [27-29]. Taken together, the effects of CQ in podocyte motility and adhesion might be helpful in maintaining normal renal filtration.

Actin cytoskeleton of podocytes could be depolymerized after CQ treatment. It may be attributed to autophagy inhibition [18, 19]. CQ is a widely used autophagy inhibitor as it suppresses autolysosomal degradation by increasing lysosomal pH [18]. Our data reveals that lysosome is an important target of CQ treatment in podocytes. There are totally 22 DEPs in which majority of them participate in intracellular degradation and turnover of proteins. Furthermore, we previously demonstrated that CQ could inhibit podocyte autophagy after 24 h treatment [18]. It is well known that autophagy is a highly conserved catabolic process which degrades unwanted cellular components to keep cell homeostasis [30]. Actin cytoskeleton is required for autophagy induction in starved cells, as it not only serves as motors for trans-

Table 2. The top 20 KEGG pathways enriched from differentially expressed proteins (DEPs) in CQ-treated podocytes

Enriched Top 20 KEGG pathways	Differentially expressed proteins (Protein ID)
Fat digestion and absorption	P04114 O14495 P02647
Fatty acid biosynthesis	O60488 O95573 P49327
Staphylococcus aureus infection	P0C0L4 P00747 P05362
Proteoglycans in cancer	P00749 Q03405 P04004 P08962 P08648 O60353 P31431 P07996 P08581 Q14573 P21333 P61812 O75369 P07711
Vitamin digestion and absorption	P04114 P02647 P41440
African trypanosomiasis	P55085 P02647 P69905 P05362 P19320
Terpenoid backbone biosynthesis	P04035 Q01581 Q13907 Q03426 P53602
Steroid biosynthesis	Q15800 Q14534 Q9UBM7 P37268 P48449
Sphingolipid metabolism	O14495 Q8NHU3 Q16739 Q13510 P06280 P17405
Cholesterol metabolism	P02649 P04114 P02749 P01130 P02647 P02656 P61916
Other glycan degradation	P04066 O00462 P07686 P06865 Q9BTY2
Glycosphingolipid biosynthesis - globo and isoglobo series	P17050 P06280 P07686 P06865
ECM-receptor interaction	P02458 P26012 P08123 P04004 Q13751 P02452 P08648 P31431 P07996 Q16787
Ferroptosis	Q13772 Q15043 P04156 P08195 Q9C0K1 P09601 Q658P3 O60488 O95573
Malaria	P69905 P60033 P07996 P05362 P19320 P08581 P25942 P61812
Protein digestion and absorption	Q96QD8 P02458 P02461 P08123 P02452 P08195 P54710 Q02388 P08473
Cell adhesion molecules (CAMs)	P26012 O95832 O95297 P10586 P31431 O14493 P05362 P28827 P19320 P25942 P32004 P14209
Complement and coagulation cascades	P0C0L4 P00750 P12259 P00747 P00749 Q03405 P04004 P01023 P00488 P00734 P15529
Lysosome	Q15012 Q9NRA2 P08962 P17050 Q13510 P61916 P06280 P04066 P07339 P50897 O00462 P17405 P53634 P10619 P07686 P07858 P07711 P06865 O14773 Q9UBR2 Q99538 O75503
Cytokine-cytokine receptor interaction	O14763 P41273 P36941 P24001 O14798 P09341 P50591 P40189 Q99988 O00300 Q9NP84 P25942 P61812

Effects of chloroquine on human podocytes

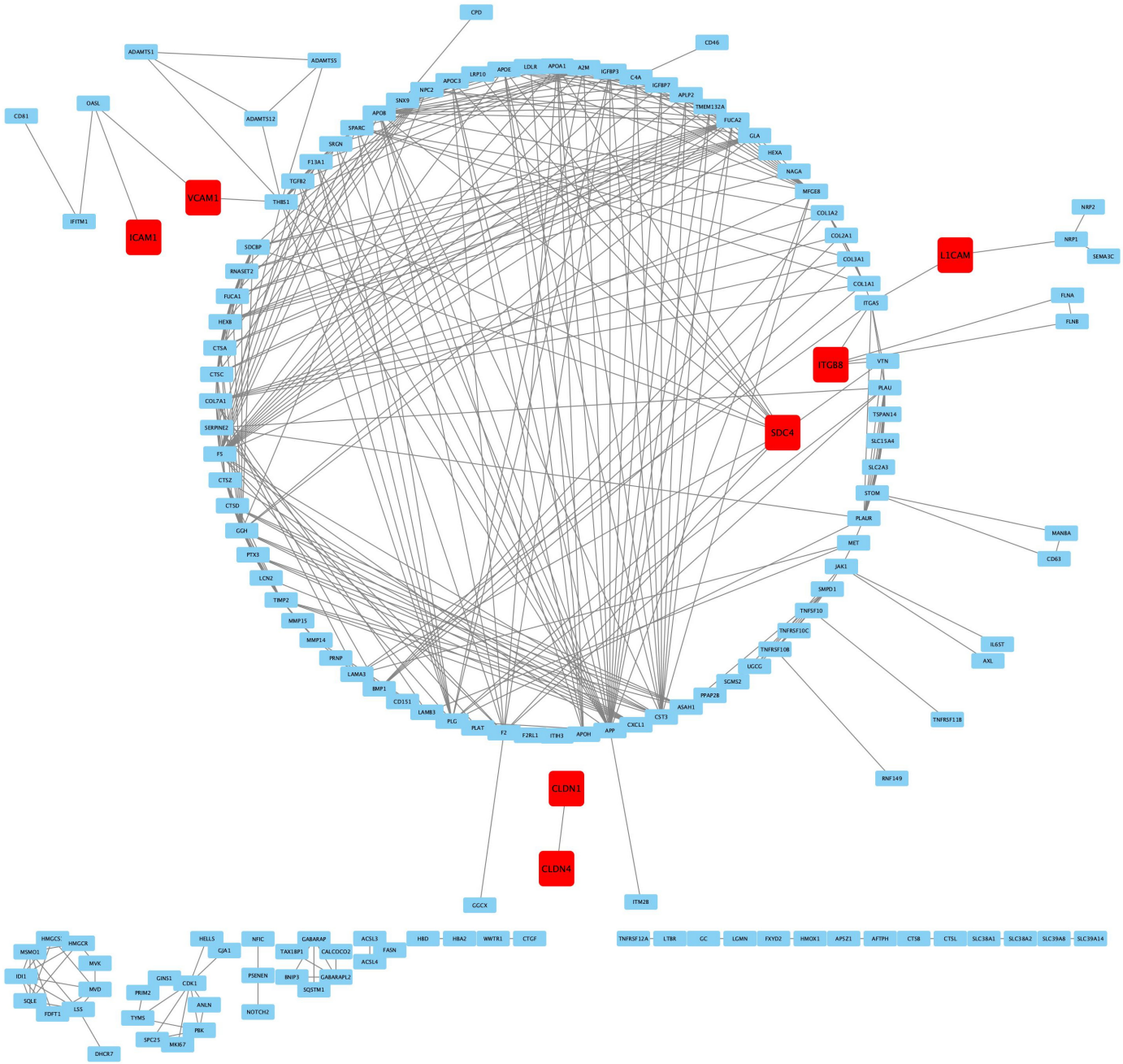

Figure 4. PPI analysis of DEPs in CQ-treated human podocytes. Totally 156 nodes and 862 edges were established in PPI network. Six cell adhesion molecules (CAMs) were founded in PPI network and highlighted in red. They are Syndecan-4, Integrin beta-8, Vascular cell adhesion protein 1, Neural cell adhesion molecule L1, Claudin-1 and Claudin-4. The node and edge represented DEP, the interaction between two DEP respectively. More edges indicated more protein interactions existed. Abbreviations: Syndecan-4, SDC4. Integrin beta-8, ITGB8. Vascular cell adhesion protein 1, VCAM1. Neural cell adhesion molecule L1, L1CAM. Claudin-1, CLDN1. Claudin-4, CLDN4.

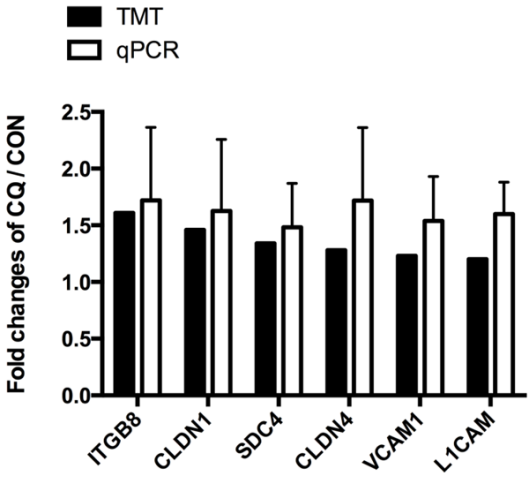

Figure 5. The mRNA expression of 6 key CAMs in human podocytes after CQ treatment. Podocytes were treated with CQ (25 μM) for 12 hours. The mRNA expressions of 6 key CAMs in podocytes were measured by real-time PCR. It showed that mRNA expressions of SDC4, ITGB8, VCAM1, L1CAM, CLDN1 and CLDN4 were consistent with results from TMT-based proteomic analysis. n=4.

porting required components but also engages in membrane invagination to form autophagosomes [31]. On the other hand, autophagy may affect the structure of actin cytoskeleton. Autophagy gene Atg7 deficient fibroblast cells present with depolymerization of actin cytoskeleton [16]. Atg7 or Atg5 mutation in kidney epithelium results in focal segmental glomeruloscerosis (FSGS) which presents with foot process enfacement in rodent models [32]. Thus, it suggested that autophagy not only protects against cell apoptosis but also may safeguard cell structure.

As for the dynamic regulators of actin cytoskeleton, three representative Rho-GTPases (RhoA, Cdc42 and Rac1) have been extensively studied in recent years [33]. For instance, podocyte-specific deletion of Cdc42 leads to severe proteinuria due to foot process effacement which was characterized by actin cytoskeleton depolymerization [34]. Similarly, foot process effacement was also presented in STZ-induced diabetic mice with podocyte-specific deletion of Rac1 [35]. Our data showed that active RhoA, Rac1 and Cdc42 decreased after CQ treatment, suggesting that they might participate in the disruption of actin cytoskeleton. In addition, our finding was also consistent with the migration assay results, as podocyte mobility is regulated by Rho-GTPases. It is known that activation of RhoA could promote podocyte motility, and over-activation or dominant negative RhoA leads to foot process effacement in rodent model [36]. Meanwhile, inactivated Cdc42 and Rac1 reduce cell motility [33]. Thus, decreased active RhoA, Rac1 and Cdc42 might be associated with actin cytoskeleton depolymerization and diminished cell motility in CQ-treated podocytes.

In summary, CQ could alter the stability of podocyte cytoskeleton. It might alleviate podocyte injury in podocytopathy by enhancing cell adhesion and diminishing podocyte motility. On the other hand, it could depolymerize actin cytoskeleton. Additionally, DEPs after CQ treatment were predominantly associated with lysosome, cell adhesion and cytokine-cytokine receptor interaction. These identified DEPs may provide new insights into the effects of CQ on human podocytes. Our findings may explain the efficacy and side effects of CQ and its analogues in treating rheumatic diseases such as lupus nephritis. Even though CQ is a recognized autophagy inhibitor, it is worth verifying whether it damages actin cytoskeleton by inhibiting autophagy. Future studies may investigate the crosstalk between autophagic proteins and actin cytoskeleton. We will explore the signaling pathways controlling podocyte motility and adhesion after CQ treatment. Further investigation on the role of identified DEPs will allow better understanding of the molecular pathways involved in CQ-treated podocytes.

Acknowledgements

We gratefully acknowledge the expert assistance of Dr. Jun-mei Zhou, Dr. Zhu-Ying Li and Dr. Yu-Jie Hu from Shanghai Children's Hospital,

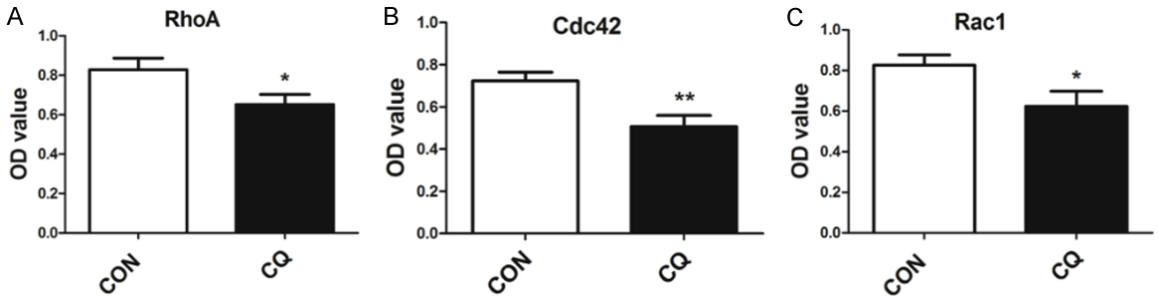

Figure 6. The active form of RhoA, Rac1 and CDC42 decreased in CQ-treated human podocytes. GTP bound (activated) RhoA, Cdc42 and Rac1 in human podocytes were measured with G-LISA assay. Theses three representative active small GTPases decreased after 24 h CQ (25 μM) treatment. **P*<0.05, ***P*<0.01 versus CON, n=6.

Shanghai Jiao Tong University in performing research experiments. This study was supported by fundings from National Natural Science Foundation of China (#81400723) and Medical excellent youth training program of Shanghai Municipal Health Bureau (#2017YQ073).

Disclosure of conflict of interest

None.

Address correspondence to: Dr. Wen-Yan Huang, Department of Nephrology and Rheumatology, Shanghai Children's Hospital, Shanghai Jiao Tong University, Shanghai 200062, China. Tel: +86-021-62474880; Fax: +86-021-62790494; E-mail: huangwenyan@sjtu.edu.cn

References

[1] Welsh GI and Saleem MA. The podocyte cytoskeleton--key to a functioning glomerulus in health and disease. Nat Rev Nephrol 2011; 8: 14-21.

[2] Faul C, Asanuma K, Yanagida-Asanuma E, Kim K and Mundel P. Actin up: regulation of podocyte structure and function by components of the actin cytoskeleton. Trends Cell Biol 2007; 17: 428-437.

[3] Feng D, DuMontier C and Pollak MR. The role of alpha-actinin-4 in human kidney disease. Cell Biosci 2015; 5: 44.

[4] Michaud JL, Hosseini-Abardeh M, Farah K and Kennedy CR. Modulating alpha-actinin-4 dynamics in podocytes. Cell Motil Cytoskeleton 2009; 66: 166-178.

[5] Nagata M. Podocyte injury and its consequences. Kidney Int 2016; 89: 1221-1230.

[6] Deegens JK, Dijkman HB, Borm GF, Steenbergen EJ, van den Berg JG, Weening JJ and Wetzels JF. Podocyte foot process effacement as a diagnostic tool in focal segmental glomerulosclerosis. Kidney Int 2008; 74: 1568-1576.

[7] Singh L, Singh G and Dinda AK. Understanding podocytopathy and its relevance to clinical nephrology. Indian J Nephrol 2015; 25: 1-7.

[8] Belingheri M, Moroni G and Messa P. Available and incoming therapies for idiopathic focal and segmental glomerulosclerosis in adults. J Nephrol 2018; 31: 37-45.

[9] Pilania RK, Jindal AK, Sandesh G, Vignesh P, Suri D, Nada R and Singh S. Chylous ascites and podocytopathy as the presentation of childhood lupus-an unusual occurrence. Lupus 2019; 28: 244-248.

[10] Srivastava T, Sharma M, Yew KH, Sharma R, Duncan RS, Saleem MA, McCarthy ET, Kats A, Cudmore PA, Alon US and Harrison CJ. LPS and PAN-induced podocyte injury in an in vitro model of minimal change disease: changes in TLR profile. J Cell Commun Signal 2013; 7: 49-60.

[11] Al-Bari MA. Chloroquine analogues in drug discovery: new directions of uses, mechanisms of actions and toxic manifestations from malaria to multifarious diseases. J Antimicrob Chemother 2015; 70: 1608-1621.

[12] Siso A, Ramos-Casals M, Bove A, Brito-Zeron P, Soria N, Munoz S, Testi A, Plaza J, Sentis J and Coca A. Previous antimalarial therapy in patients diagnosed with lupus nephritis: influence on outcomes and survival. Lupus 2008; 17: 281-288.

[13] Spinelli FR, Moscarelli E, Ceccarelli F, Miranda F, Perricone C, Truglia S, Garufi C, Massaro L, Morello F, Alessandri C, Valesini G and Conti F. Treating lupus patients with antimalarials: analysis of safety profile in a single-center cohort. Lupus 2018; 27: 1616-1623.

[14] Imaizumi T, Hayakari R, Matsumiya T, Yoshida H, Tsuruga K, Watanabe S, Kawaguchi S and Tanaka H. Chloroquine attenuates TLR3/IFN-beta signaling in cultured normal human mesangial cells: a possible protective effect against renal damage in lupus nephritis. Mod Rheumatol 2017; 27: 1004-1009.

[15] Muller-Hocker J, Schmid H, Weiss M, Dendorfer U and Braun GS. Chloroquine-induced phospholipidosis of the kidney mimicking Fabry's

disease: case report and review of the literature. Hum Pathol 2003; 34: 285-289.
[16] Zhuo C, Ji Y, Chen Z, Kitazato K, Xiang Y, Zhong M, Wang Q, Pei Y, Ju H and Wang Y. Proteomics analysis of autophagy-deficient Atg7-/-MEFs reveals a close relationship between F-actin and autophagy. Biochem Biophys Res Commun 2013; 437: 482-488.
[17] Saleem MA, O'Hare MJ, Reiser J, Coward RJ, Inward CD, Farren T, Xing CY, Ni L, Mathieson PW and Mundel P. A conditionally immortalized human podocyte cell line demonstrating nephrin and podocin expression. J Am Soc Nephrol 2002; 13: 630-638.
[18] Kang YL, Saleem MA, Chan KW, Yung BY and Law HK. The cytoprotective role of autophagy in puromycin aminonucleoside treated human podocytes. Biochem Biophys Res Commun 2014; 443: 628-634.
[19] Kang YL, Saleem MA, Chan KW, Yung BY and Law HK. Trehalose, an mTOR independent autophagy inducer, alleviates human podocyte injury after puromycin aminonucleoside treatment. PLoS One 2014; 9: e113520.
[20] Peti-Peterdi J and Sipos A. A high-powered view of the filtration barrier. J Am Soc Nephrol 2010; 21: 1835-1841.
[21] Neal CR, Crook H, Bell E, Harper SJ and Bates DO. Three-dimensional reconstruction of glomeruli by electron microscopy reveals a distinct restrictive urinary subpodocyte space. J Am Soc Nephrol 2005; 16: 1223-1235.
[22] Neal CR, Muston PR, Njegovan D, Verrill R, Harper SJ, Deen WM and Bates DO. Glomerular filtration into the subpodocyte space is highly restricted under physiological perfusion conditions. Am J Physiol Renal Physiol 2007; 293: F1787-1798.
[23] Saito K, Shiino T, Kurihara H, Harita Y, Hattori S and Ohta Y. Afadin regulates RhoA/Rho-associated protein kinase signaling to control formation of actin stress fibers in kidney podocytes. Cytoskeleton (Hoboken) 2015; 72: 146-156.
[24] Mouawad F, Tsui H and Takano T. Role of Rho-GTPases and their regulatory proteins in glomerular podocyte function. Can J Physiol Pharmacol 2013; 91: 773-782.
[25] Norgaard JC, Stengaard-Pedersen K, Norgaard M and de Thurah A. Antimalarials in the treatment of systemic lupus erythematosus: a registry-based cohort study in Denmark. Lupus 2015; 24: 299-306.
[26] Liu Y, Echtermeyer F, Thilo F, Theilmeier G, Schmidt A, Schulein R, Jensen BL, Loddenkemper C, Jankowski V, Marcussen N, Gollasch M, Arendshorst WJ and Tepel M. The proteoglycan syndecan 4 regulates transient receptor potential canonical 6 channels via RhoA/Rho-associated protein kinase signaling. Arterioscler Thromb Vasc Biol 2012; 32: 378-385.
[27] Elangbam CS, Qualls CW Jr and Dahlgren RR. Cell adhesion molecules--update. Vet Pathol 1997; 34: 61-73.
[28] Tsukita S and Furuse M. The structure and function of claudins, cell adhesion molecules at tight junctions. Ann N Y Acad Sci 2000; 915: 129-135.
[29] Liddelow S and Hoyer D. Astrocytes: adhesion molecules and immunomodulation. Curr Drug Targets 2016; 17: 1871-1881.
[30] De Rechter S, Decuypere JP, Ivanova E, van den Heuvel LP, De Smedt H, Levtchenko E and Mekahli D. Autophagy in renal diseases. Pediatr Nephrol 2016; 31: 737-752.
[31] Zientara-Rytter K and Subramani S. Role of actin in shaping autophagosomes. Autophagy 2016; 12: 2512-2515.
[32] Kawakami T, Gomez IG, Ren S, Hudkins K, Roach A, Alpers CE, Shankland SJ, D'Agati VD and Duffield JS. Deficient autophagy results in mitochondrial dysfunction and FSGS. J Am Soc Nephrol 2015; 26: 1040-1052.
[33] Ding WY and Saleem MA. Current concepts of the podocyte in nephrotic syndrome. Kidney Res Clin Pract 2012; 31: 87-93.
[34] Blattner SM, Hodgin JB, Nishio M, Wylie SA, Saha J, Soofi AA, Vining C, Randolph A, Herbach N, Wanke R, Atkins KB, Gyung Kang H, Henger A, Brakebusch C, Holzman LB and Kretzler M. Divergent functions of the Rho GTPases Rac1 and Cdc42 in podocyte injury. Kidney Int 2013; 84: 920-930.
[35] Ishizaka M, Gohda T, Takagi M, Omote K, Sonoda Y, Oliva Trejo JA, Asao R, Hidaka T, Asanuma K, Horikoshi S and Tomino Y. Podocyte-specific deletion of Rac1 leads to aggravation of renal injury in STZ-induced diabetic mice. Biochem Biophys Res Commun 2015; 467: 549-555.
[36] Asanuma K, Yanagida-Asanuma E, Faul C, Tomino Y, Kim K and Mundel P. Synaptopodin orchestrates actin organization and cell motility via regulation of RhoA signalling. Nat Cell Biol 2006; 8: 485-491.

Supplementary Material-1

All identified DEPs in human podocytes after CQ treatment. Totally 277 DEPs (210 up-regulated and 67 down-regulated) were identified in podocytes after CQ treatment (25 μM) for 24 hour. The value of CQ/Control indicated the fold changes of protein after CQ treatment. $P<0.05$ was considered statistically significant.